AD-A048 037 ROME AIR DEVELOPMENT CENTER GRIFFISS AFB N Y F/G 10/2
RADIATION EFFECTS ON AlGAAS/GAAS SOLAR CELLS USING 0.9-3.0 MEV --ETC(U)
SEP 77 L F LOWE, J R CAPPELLI, L W JAMES

UNCLASSIFIED RADC-TR-77-332 NL

| OF |
AD
A048 037

END
DATE
FILMED
1 -78
DDC

RADC-TR-77-332
IN-HOUSE REPORT
SEPTEMBER 1977

Radiation Effects on AlGaAs/GaAs Solar Cells Using 0.9 - 3.0 MeV Protons and 1.0 - 1.4 MeV Electrons

L.F. LOWE
J.R. CAPPELLI
L.W. JAMES
R.L. MOON

Approved for public release; distribution unlimited.

ROME AIR DEVELOPMENT CENTER
AIR FORCE SYSTEMS COMMAND
GRIFFISS AIR FORCE BASE, NEW YORK 13441

This report has been reviewed by the RADC Information Office (OI) and is releasable to the National Technical Information Service (NTIS). At NTIS it will be releasable to the General public, including foreign nations.

This technical report has been reviewed and approved for publication.

APPROVED:

BOBBY L. BUCHANAN, Chief
Radiation Hardened Electronics Technology

APPROVED:

ROBERT M. BARRETT, Director
Solid State Sciences Division

FOR THE COMMANDER:

Plans Office

Unclassified

SECURITY CLASSIFICATION OF THIS PAGE (When Data Entered)

REPORT DOCUMENTATION PAGE

READ INSTRUCTIONS BEFORE COMPLETING FORM

1. REPORT NUMBER: RADC-TR-77-332	2. GOVT ACCESSION NO.
	3. RECIPIENT'S CATALOG NUMBER: Technical rept.
4. TITLE (and Subtitle): RADIATION EFFECTS ON AlGaAs/GaAs SOLAR CELLS USING Ø.9 - 3.Ø MeV PROTONS AND 1.Ø - 1.4 MeV ELECTRONS	5. TYPE OF REPORT & PERIOD COVERED: ~~Scientific Report~~ 1 Jan. -31 Dec [redacted]76
	6. PERFORMING ORG. REPORT NUMBER
7. AUTHOR(s): L. F. Lowe, J. R. Cappelli, L. W. James*, R. L. Moon	8. CONTRACT OR GRANT NUMBER(s)
9. PERFORMING ORGANIZATION NAME AND ADDRESS: Deputy for Electronic Technology (RADC/ESR) Hanscom AFB Massachusetts 01731	10. PROGRAM ELEMENT, PROJECT, TASK AREA & WORK UNIT NUMBERS: 62702F 46002001
11. CONTROLLING OFFICE NAME AND ADDRESS: Deputy for Electronic Technology (RADC/ESR) Hanscom AFB Massachusetts 01731	12. REPORT DATE: Sept[redacted] 1977
	13. NUMBER OF PAGES: 33
14. MONITORING AGENCY NAME & ADDRESS (if different from Controlling Office): 33p.	15. SECURITY CLASS. (of this report): Unclassified
	15a. DECLASSIFICATION/DOWNGRADING SCHEDULE

16. DISTRIBUTION STATEMENT (of this Report)

Approved for public release; distribution unlimited.

17. DISTRIBUTION STATEMENT (of the abstract entered in Block 20, if different from Report)

18. SUPPLEMENTARY NOTES

*Varian Associates, Palo Alto, California

19. KEY WORDS (Continue on reverse side if necessary and identify by block number)

(1) Solar cells
(2) AlGaAs
(3) Radiation effects
(4) Space environment

20. ABSTRACT (Continue on reverse side if necessary and identify by block number)

Aluminum gallium arsenide solar cells were irradiated with 1.0 and 1.4 MeV electrons, and with 0.9 and 3.0 MeV protons to determine radiation sensitivity. Electron fluences ranged from 1×10^{14} to 3×10^{16} electrons cm^{-2}, and proton fluences from 5×10^{10} to 2.7×10^{12} cm^{-2}. A solar simulator and a tungsten lamp were used to evaluate changes in the current-voltage characteristic curves. In most cases, AlGaAs solar cells showed a greater resistance to radiation than silicon cells.

10 to the 12th power /sqcm

DD FORM 1 JAN 73 1473 EDITION OF 1 NOV 65 IS OBSOLETE

Unclassified

SECURITY CLASSIFICATION OF THIS PAGE (When Data Entered)

10 to the 14th power
10 to the 16th power
10 to the 10th power

/sqcm

309 050

LB

Unclassified

SECURITY CLASSIFICATION OF THIS PAGE(When Data Entered)

Unclassified

SECURITY CLASSIFICATION OF THIS PAGE(When Data Entered)

Preface

The authors thank Roger Little and John Menucci of Simulation Physics, Inc. for their assistance in the solar simulator and tungsten lamp measurements.

Preceding Page Blank - NOT FILMED

Contents

Illustrations

Tables

Radiation Effects on AlGaAs/GaAs Solar Cells Using 0.9 – 3.0 MeV Protons and 1.0 – 1.4 MeV Electrons

1. INTRODUCTION

In order to evaluate the applicability of AlGaAs for use as a solar cell material, information is needed on its sensitivity to the radiation that they would be exposed to in space. To this end AlGaAs solar cells were exposed to 1.0 and 1.4 MeV electrons, and 0.9 and 3.0 MeV protons. The electron fluences ranged from 1×10^{14} to 3×10^{16} electrons cm^{-2}, and the proton fluences ranged from 5×10^{10} to 2.7×10^{12} protons cm^{-2}.

2. EXPERIMENTAL

Cells were fabricated by conventional LPE processes, where the p-type AlGaAs (AlAs - 0.80) was grown on an n-type GaAs(111)B substrate. During growth, the p-dopant diffused into the n-layer to form a p-n junction approximately 0.3 to 0.8 micron deep in the GaAs. Doping densities of the p-AlGaAs + n-GaAs substrate were 3×10^{18} cm^{-3} and 8×10^{17} cm^{-3}, respectively. A p-type GaAs layer was grown on top of the AlGaAs in order to facilitate contacting, and later removed by a selective etch using the contact grid as a mask. Cell area was 1.613 cm^2. These cells were *not* optimized for air mass zero (AMO) performance,

(Received for publication 29 September 1977)

since the AlGaAs were generally too thick, reducing the blue response. SiO_2 deposited to a thickness of 750 Å was used as an antireflection coating. AMO efficiencies were 10-12 percent. Proton irradiation experiments were conducted at the Van de Graaff facility at RADC/ET, Massachusetts. After each irradiation to a given fluence, the I-V curve was measured using an AMO solar simulator and a tungsten lamp as light source. Proton energies of 0.9 and 3 MeV were used, up to maximum fluences of 5×10^{11} p/cm^2 and 3×10^{12} p/cm^2, respectively.

Electron bombardment was carried out at the Dynamitron accelerator at RADC/ET, Massachusetts. Electron energies of 1 and 1.4 MeV were used up to maximum fluence of 3×10^{16} e/cm^2 and 3×10^{15} e/cm^2, respectively. AMO data were taken using Spectrolab solar simulators at these locations. All measurements were taken at 25°C.

After initial characterization, all samples were evaluated for radiation induced changes in their current-voltage (i-v) characteristic curves using both a solar simulator at AMO and also a tungsten lamp. After each tungsten run, the tungsten intensity was adjusted so as to bring the short circuit current back to what it was before any irradiation (I_{sco}). In addition after the final irradiation, the spectral response was determined for each cell. The individual irradiation procedures were as follows.

3. ELECTRONS

The electron irradiations were made using a 1.5 MeV Dynamitron electron accelerator. Two samples each were mounted on either side of the aperture of a Faraday cup so that all fluences were measured directly. The cells were open circuited during the irradiation and the exposures were carried out at room temperature in air. The electron flux was approximately 10^{12} electrons cm^{-2} s^{-1}. Two energies were used, 1.0 and 1.4 MeV.

4. PROTONS

A 3.0 MeV Van de Graaff accelerator was used for the proton exposures. Because of the short range of protons these experiments were carried out in vacuum, one cell at a time. Each cell was mounted in the center of a Faraday cup which was part of the vacuum system. A collimator, electrically isolated from the Faraday cup, defined the exposure area. The Van de Graaff is equipped with a beam sweeping device which leads to an exposure uniformity of better than 10 percent. Proton flux levels were 10^{10} protons cm^{-2} s^{-1}, and runs were made open circuited at 0.9 and 3.0 MeV.

5. RESULTS

Figures 1-8 give the individual I-V curves as a function of fluence using the solar simulator at AMO. Figures 9-16 show tungsten lamp data for the same exposures. Figures 17-21 illustrate the effect of increasing the tungsten lamp intensity so as to bring the cell output current back to its preirradiation value (the I_{sco} case). Contact problems were encountered with 3 cells. Pertinent data from Figures 1-16 are given in Tables 1-8, including the incomplete data for the three cells with contact problems. The output power data is shown in Figures 22-26. After two weeks, the cells were checked for annealing. None was observed. Spectral response data are shown in Figures 27-30.

6. SUMMARY AND DISCUSSION

Solar cells of p-AlGaAs/n-GaAs were subjected to 0.9 and 3 MeV proton radiation, and 1 and 1.4 MeV electron radiation. Values of critical fluence ϕ_c at which the output power was reduced by 25 percent were determined. As expected protons with energies of 0.9 MeV caused the most severe degradation, and a $\phi_c = 4 \times 10^{10}$ p/cm^2 was determined. Fortunately because of the short range of low energy protons, this type of radiation can be protected against by cover slips. For 3 MeV protons, $\phi_c = 5 \times 10^{11}$ p/cm^2.

Critical fluences for 1.4 MeV electrons were 7-9 $\times 10^{14}$ e/cm^2. A total of five cells were irradiated at electron energies of 1 MeV. ϕ_c varied between 7×10^{14} and 7×10^{15} e/cm^2. At fluences $<10^{15}$ e/cm^2, the relative cell parameters followed the characteristic radiation equation. At fluences greater than this the relative parameters varied linearly with $\ln\phi$, as did the relative diffusion length.

These results show that the radiation resistance of AlGaAs/GaAs solar cells is equal to or better than that observed in conventional and violet Si cells for all the radiation fluxes investigated here, except 0.9 MeV protons. In the case of 1 MeV electrons, the value of $\phi_c = 7 \times 10^{15}$ e/cm^2 is believed to be the highest observed for conventional cells. The spread in ϕ_c we observed is thought to be caused by variations in junction depth, which can be optimized. So even for 1 MeV electrons, cells of AlGaAs/GaAs are superior to those of Si.

Computer calculations show that the variation in I_{sc} as a function of irradiation level is sensitive to junction depth. Thus a shallow junction solar cell should be more radiation-resistant than the experimental data shown here, since I_{sc} does not change as rapidly with decreasing diffusion length as in a deep junction device.

Calculations also demonstrated that the AMO efficiency increases with AlAs concentration in the AlGaAs for a given thickness. This will allow operation in concentrated sunlight in the space environment because the sheet resistance of the AlGaAs can be reduced without substantially degrading performance through optical absorption of high energy protons in the contact layer.

Combining the radiation resistance characteristics with the ability to obtain AMO efficiencies of 16 percent, and potentially 18 percent, makes the AlGaAs/GaAs solar cells attractive for space applications.

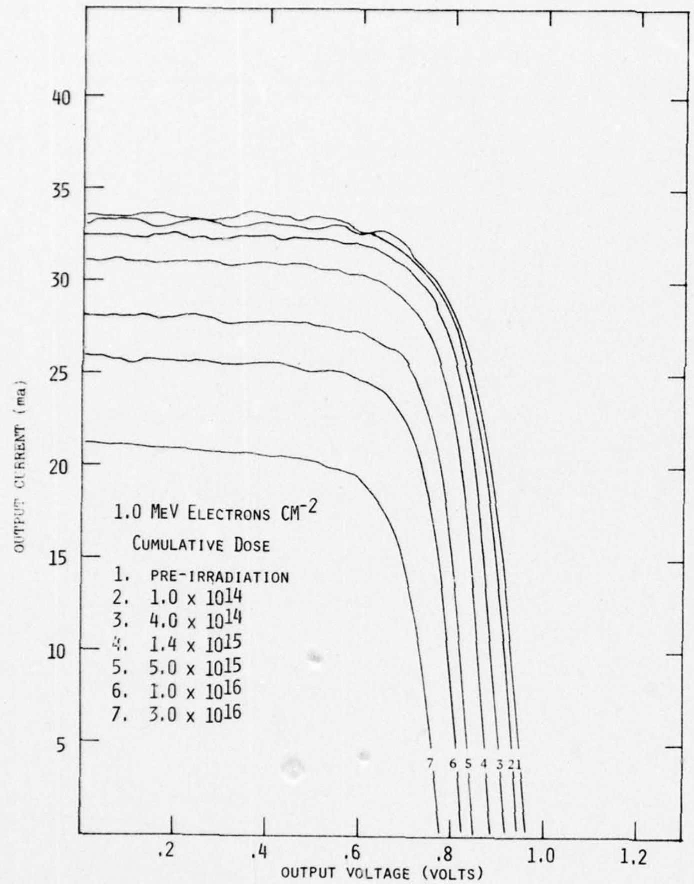

Figure 1. Power Output of Cell No. 10-7-75B, Solar Simulator at AMO

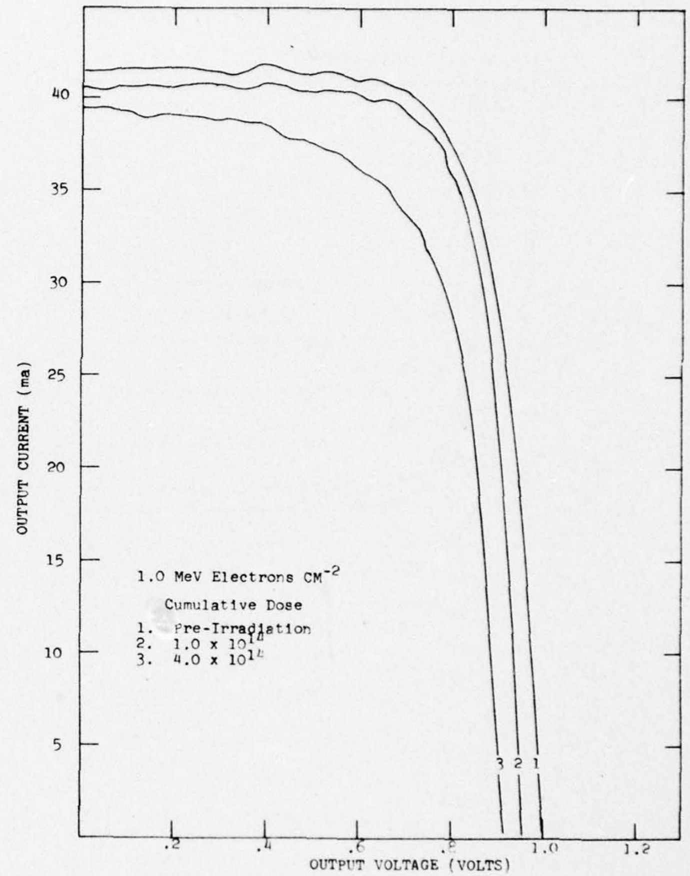

Figure 2. Power Output of Cell No. 9-23-75B Solar Simulator at AMO

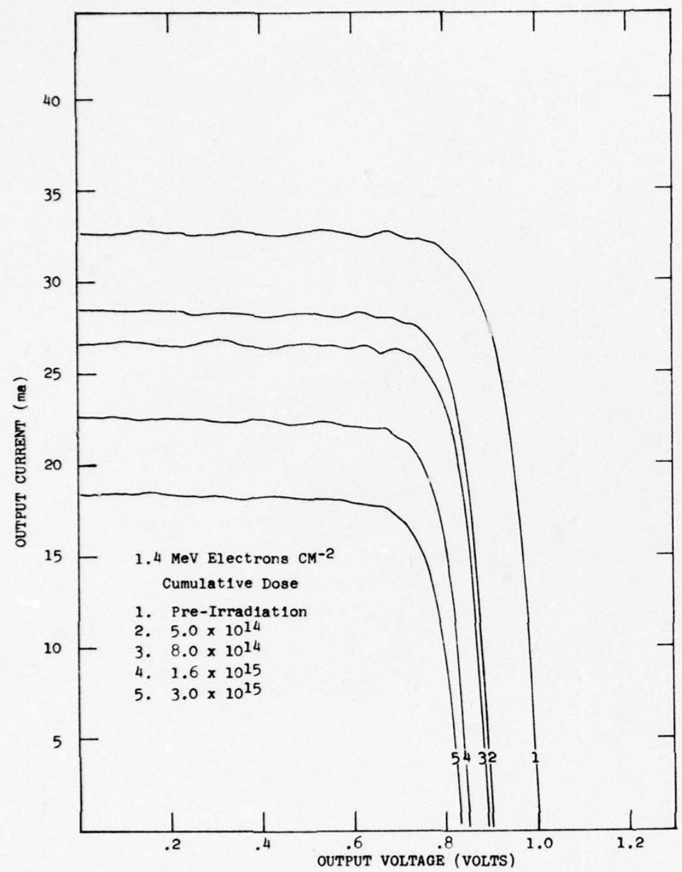

Figure 3. Power Output of Cell No. 1-26-76B, Solar Simulator at AMO

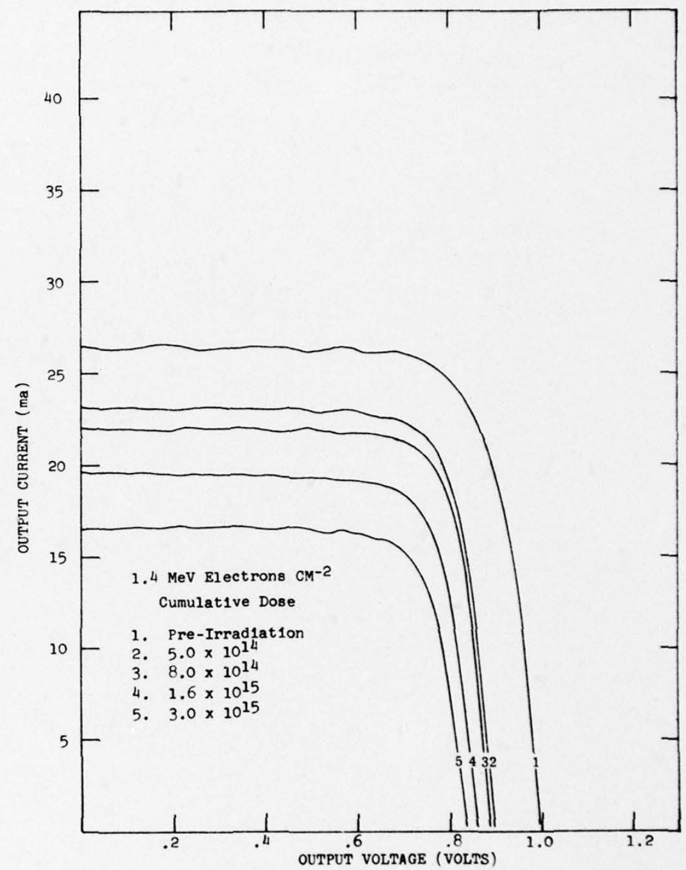

Figure 4. Power Output of Cell No. 1-22-76B, Solar Simulator at AMO

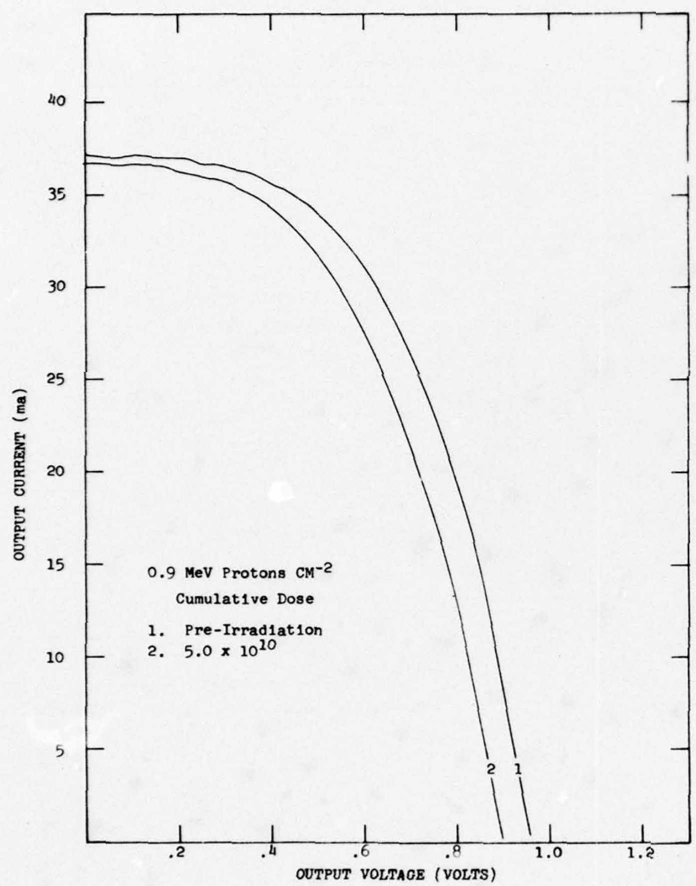

Figure 5. Power Output of Cell No. 9-15-75C, Solar Simulator at AMO

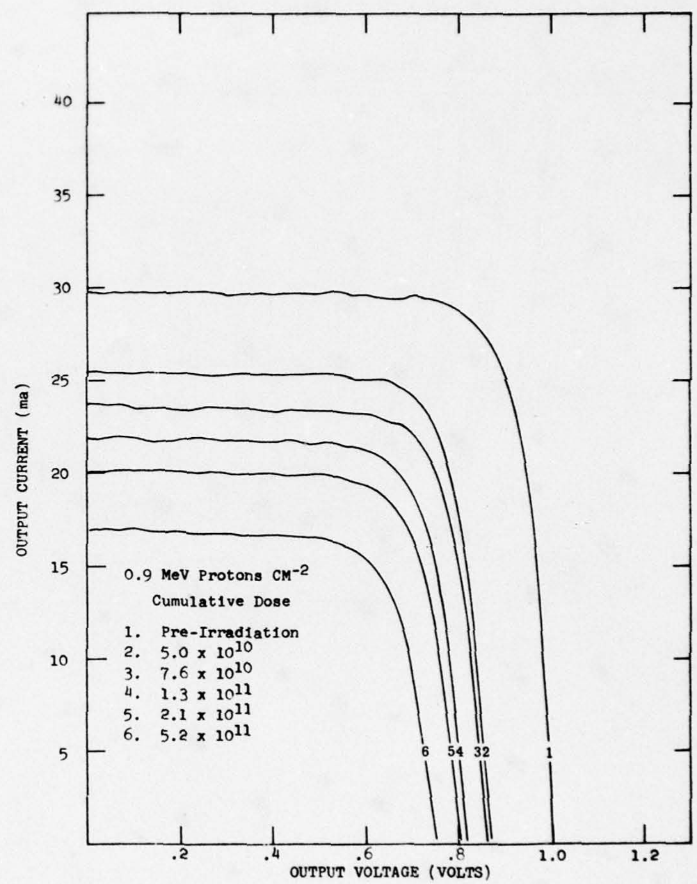

Figure 6. Power Output of Cell No. 2-4-76B, Solar Simulator at AMO

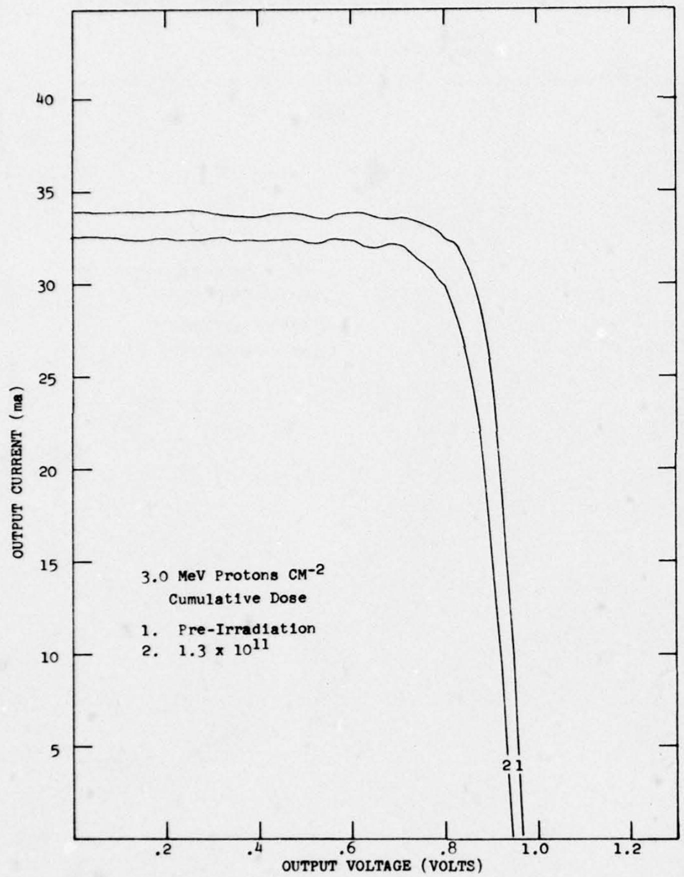

Figure 7. Power Output of Cell No. 1-30-76D, Solar Simulator at AMO

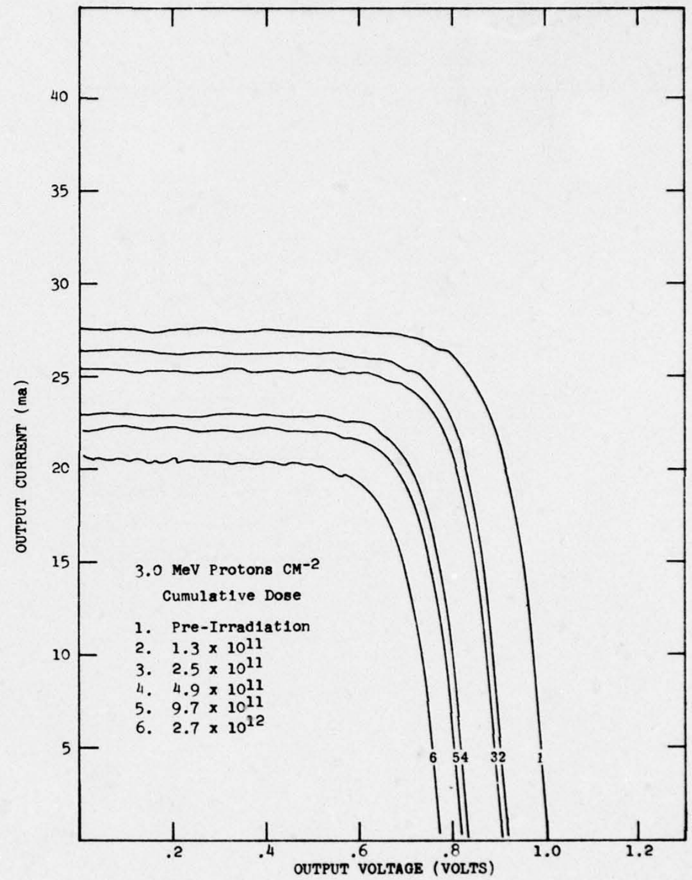

Figure 8. Power Output of Cell No. 3-2-76A, Solar Simulator at AMO

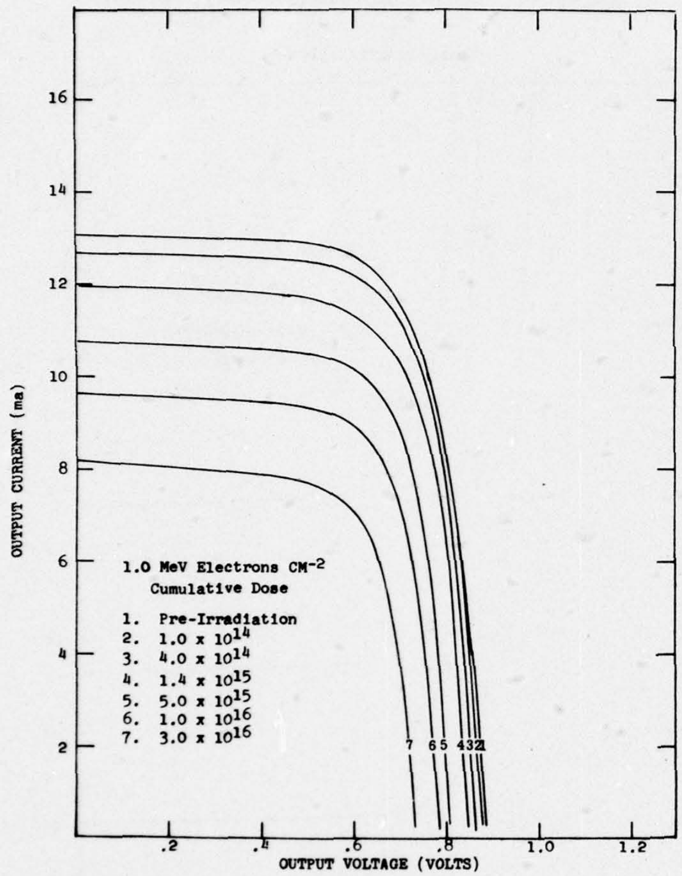

Figure 9. Power Output of Cell No. 10-7-75B, Tungsten Lamp

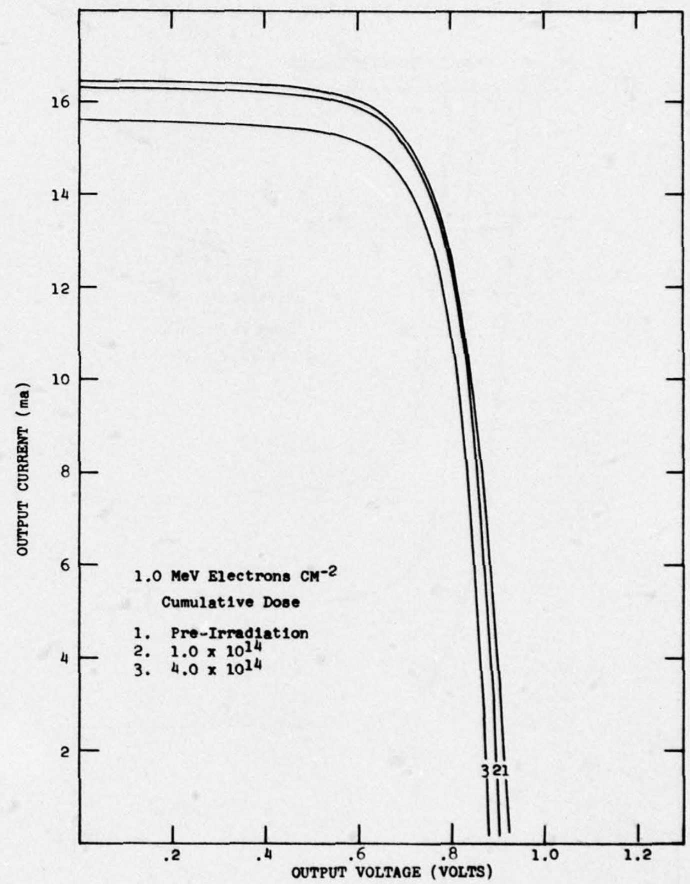

Figure 10. Power Output of Cell No. 9-23-75B, Tungsten Lamp

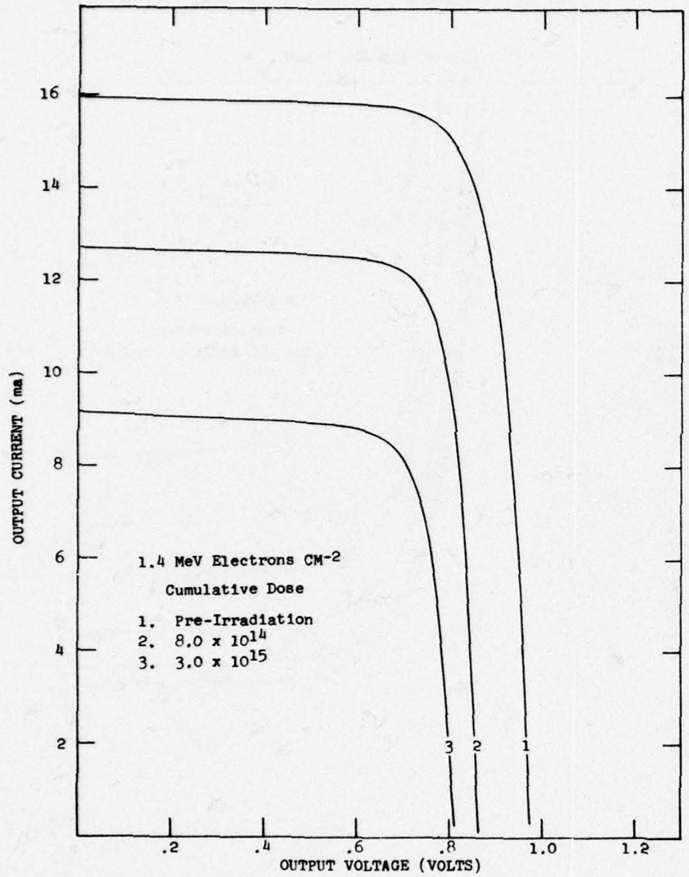

Figure 11. Power Output of Cell No. 1-26-76B, Tungsten Lamp

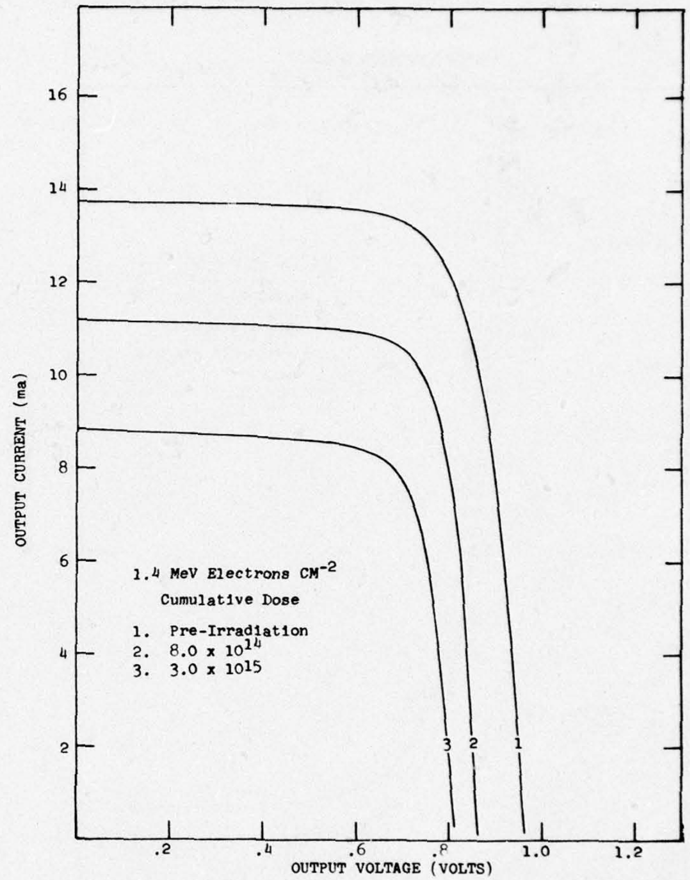

Figure 12. Power Output of Cell No. 1-22-76B, Tungsten Lamp

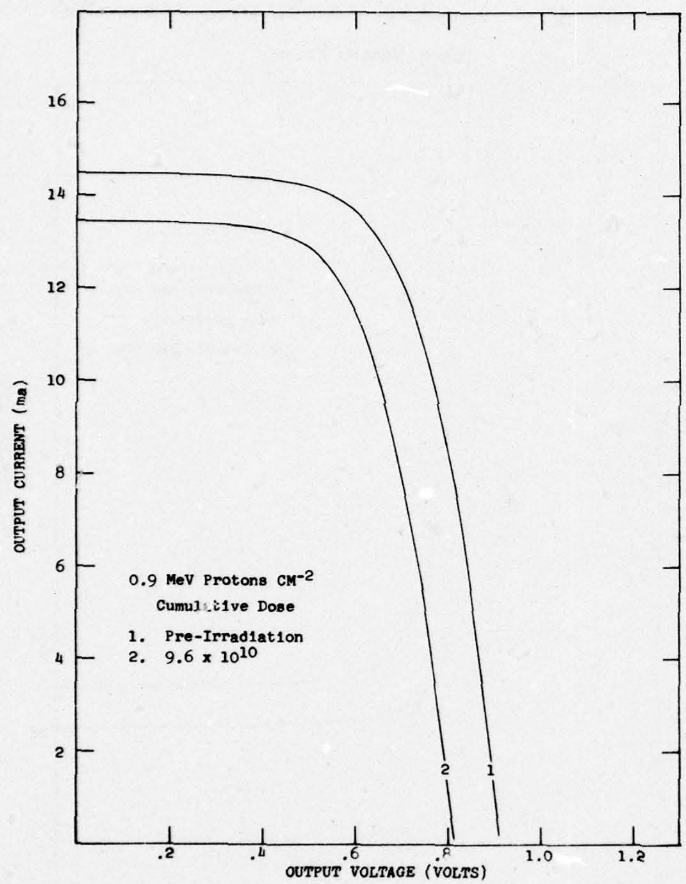

Figure 13. Power Output of Cell No. 9-15-75C, Tungsten Lamp

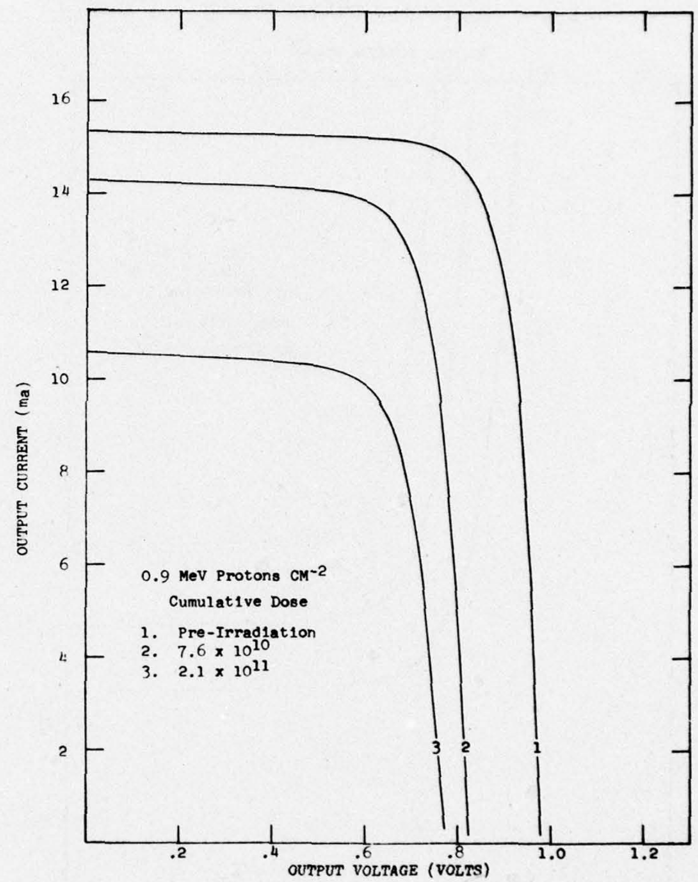

Figure 14. Power Output of Cell No. 2-4-76B, Tungsten Lamp

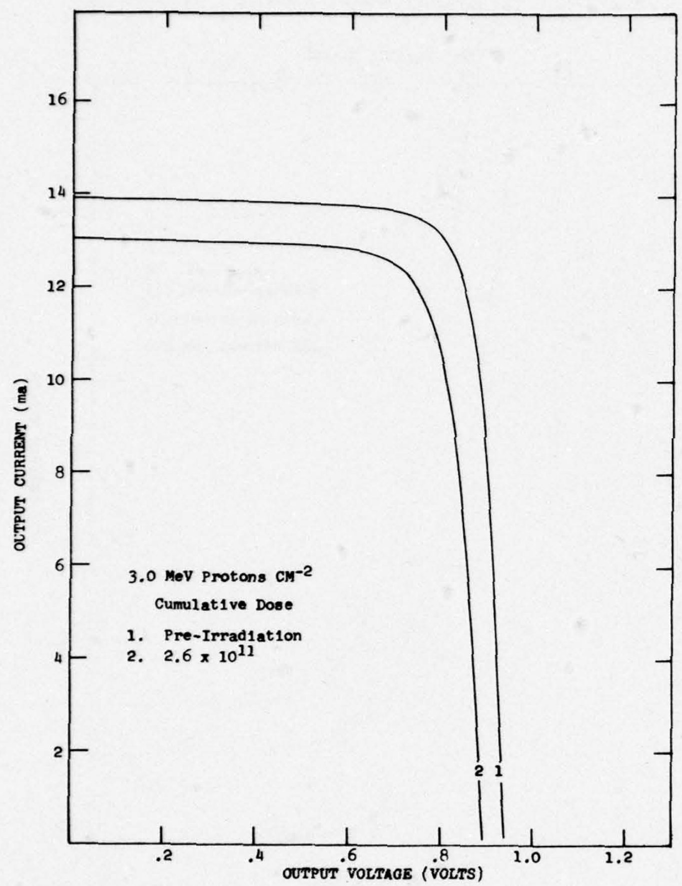

Figure 15. Power Output of Cell No. 1-30-76D, Tungsten Lamp

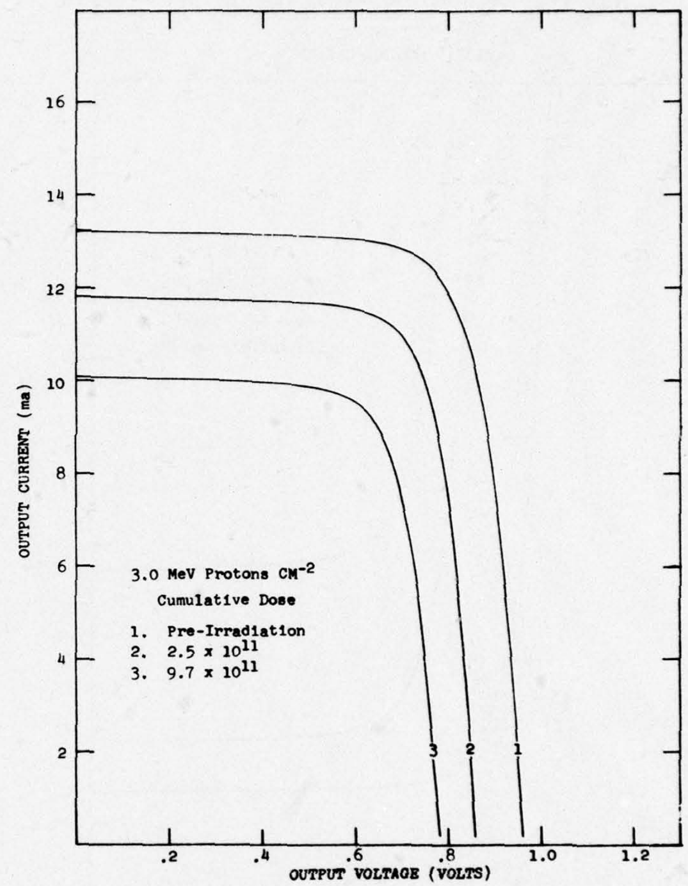

Figure 16. Power Output of Cell No. 3-2-76A, Tungsten Lamp

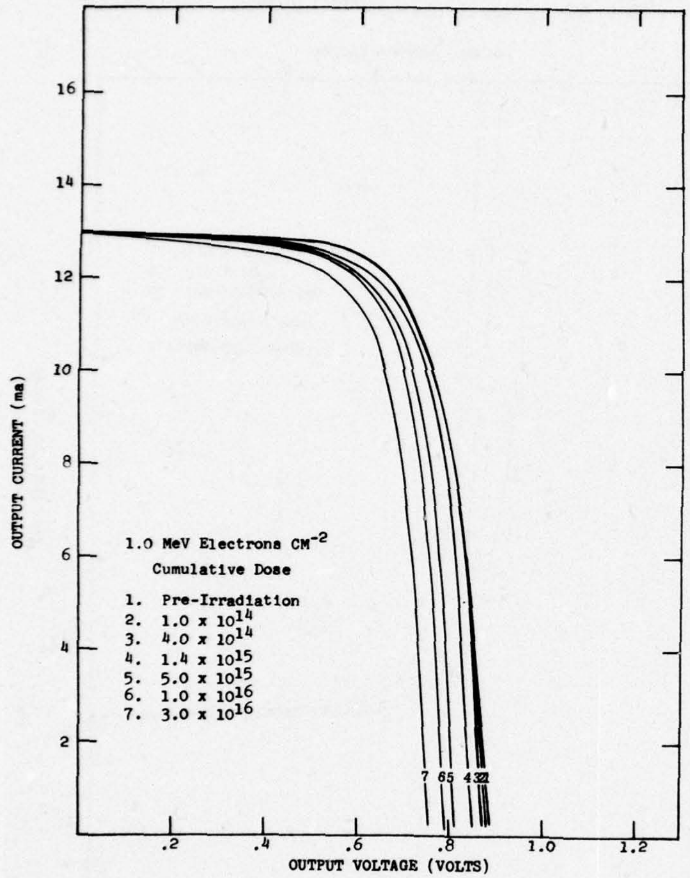

Figure 17. Power Output of Cell No. 10-7-75B, Tungsten Lamp, I_{sco} Case

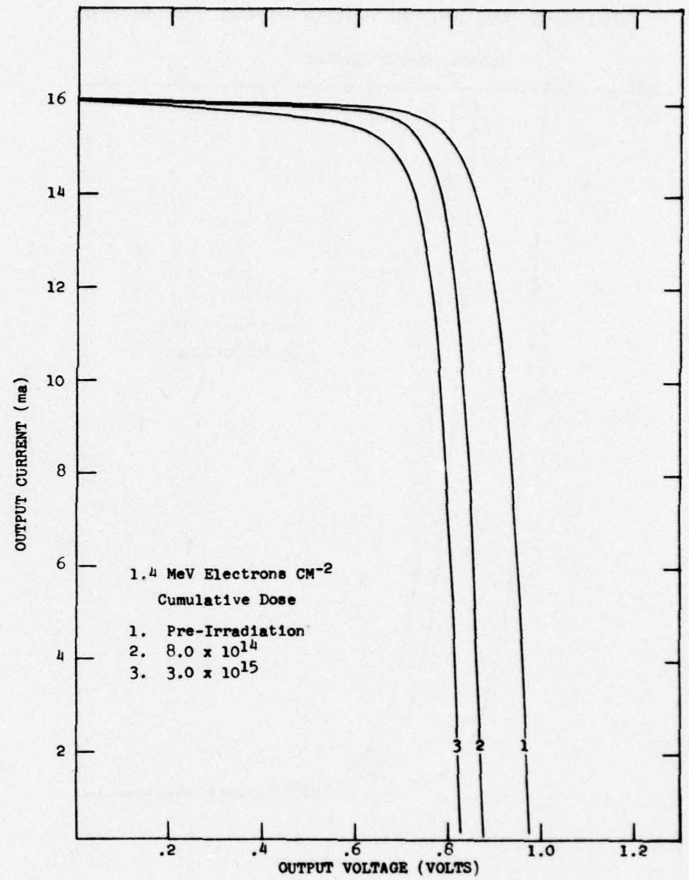

Figure 18. Power Output of Cell No. 1-26-76B, Tungsten Lamp, I_{sco} Case

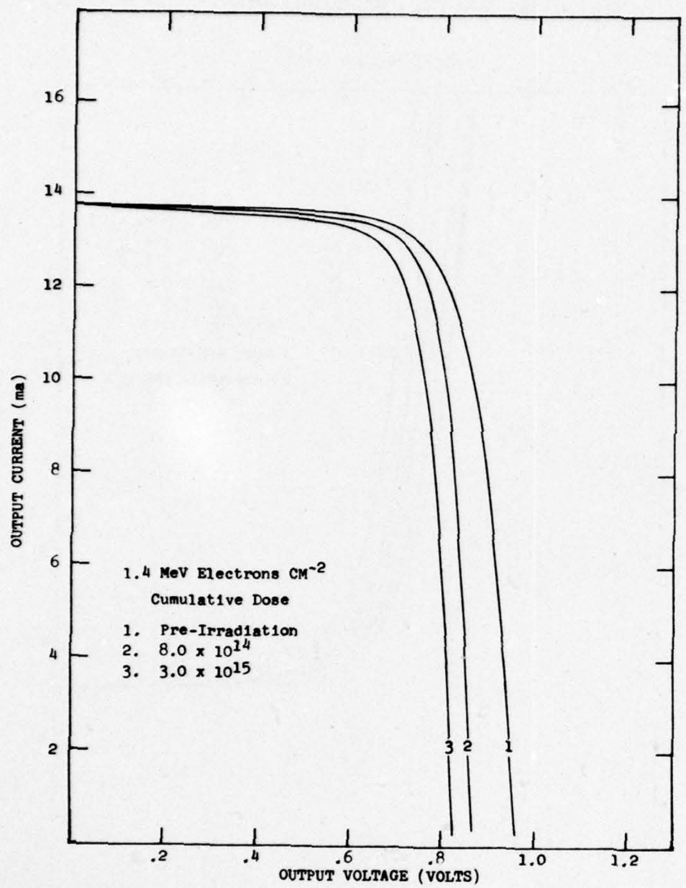

Figure 19. Power Output of Cell No. 1-22-76B, Tungsten Lamp, I_{sco} Case

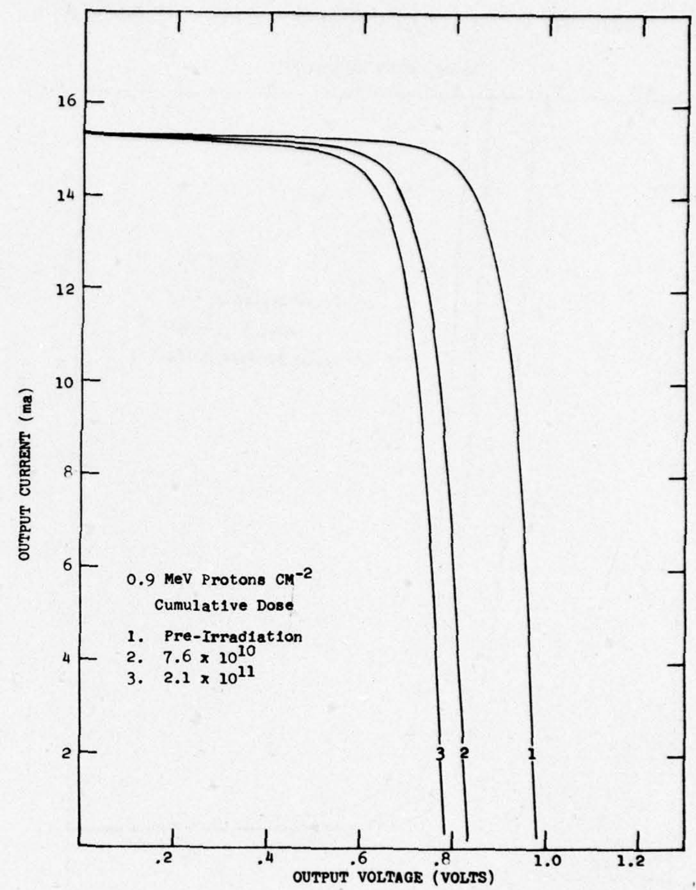

Figure 20. Power Output of Cell No. 2-4-76B, Tungsten Lamp, I_{sco} Case

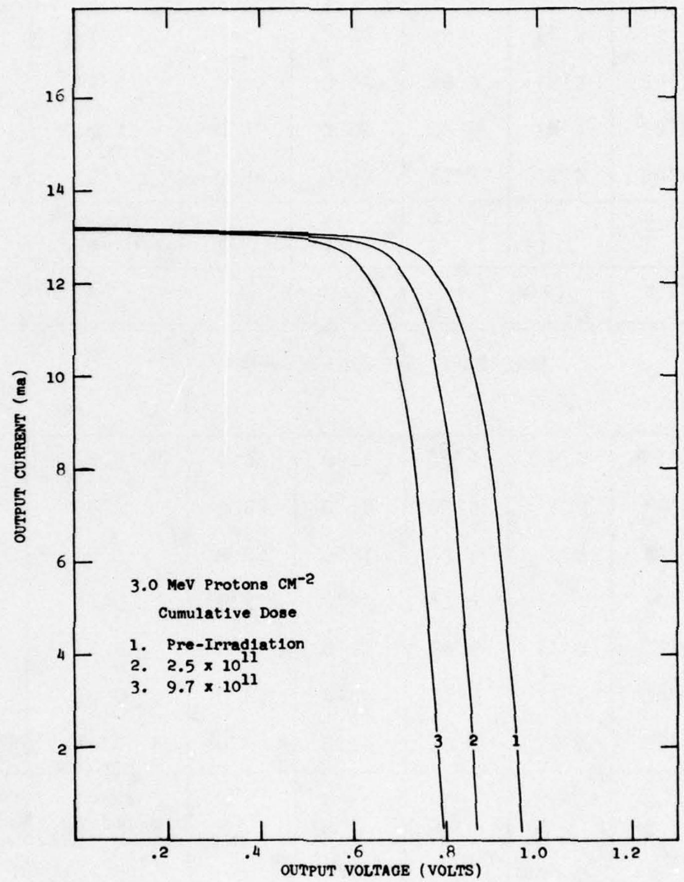

Figure 21. Power Output of Cell No. 3-2-76A, Tungsten Lamp, I_{sco} Case

Table 1. Cell No. 10-7-75B

$e^- cm^{-2}$	I_{sc} (mA)		V_{oc} (volts)		P_{ep} (mw)		P_{max} (mw)		Fill Factor	
	Solar Simulator	Tungsten Lamp	S S	T L	S S	T L	S S	T L	S S	T L
0	33.5	13.0	0.96	0.89	32.2	11.6	22.8	8.1	0.708	0.698
1.0×10^{14}	33.0	13.0	0.94	0.88	31.0	11.4	22.6	8.1	0.729	0.711
4.0×10^{14}	32.5	12.6	0.91	0.87	29.6	11.0	22.0	7.8	0.743	0.709
1.4×10^{15}	31.1	11.9	0.88	0.85	27.4	10.1	20.3	7.3	0.741	0.723
5.0×10^{15}	28.0	10.7	0.85	0.81	23.8	8.7	17.9	6.4	0.752	0.736
1.0×10^{16}	26.0	9.7	0.82	0.78	21.3	7.6	15.7	5.4	0.737	0.711
3.0×10^{16}	21.3	8.2	0.77	0.74	16.4	6.1	11.6	4.3	0.707	0.705

Table 2. Cell No. 9-23-75B

$e^- cm^{-2}$	I_{sc} (mA)		V_{oc} (volts)		P_{ep} (mw)		P_{max} (mw)		Fill Factor	
	Solar Simulator	Tungsten Lamp	S S	T L	S S	T L	S S	T L	S S	T L
0	41.5	16.5	0.99	0.92	41.1	15.2	30.0	10.7	0.730	0.704
1.0×10^{14}	40.5	16.3	0.96	0.90	38.9	14.7	28.9	10.7	0.743	0.728
4.0×10^{14}	39.5	15.6	0.91	0.88	35.9	13.7	24.1	10.0	0.671	0.730
1.4×10^{15}	35.5	14.5	--	0.82	--	11.9	--	--	--	--
2.5×10^{16}	19.5	--	0.78	--	15.4	--	11.3	--	0.734	--

Table 3. Cell No. 1-26-76B

$e^- cm^{-2}$	I_{sc} (mA)		V_{oc} (volts)		P_{ep} (mw)		P_{max} (mw)		Fill Factor	
	Solar Simulator	Tungsten Lamp	S S	T L	S S	T L	S S	T L	S S	T L
0	32.6	15.9	1.0	0.97	32.6	15.4	25.8	12.1	0.791	0.786
5.0×10^{14}	28.5	--	0.90	--	25.7	--	20.5	--	0.798	--
8.0×10^{14}	26.6	12.7	0.89	0.86	23.7	10.9	19.0	8.7	0.802	0.798
1.6×10^{15}	22.6	--	0.85	--	19.2	--	15.1	--	0.786	--
3.0×10^{15}	18.4	9.2	0.83	0.81	15.3	7.5	11.9	5.7	0.778	0.760

Table 4. Cell No. 1-22-76B

$e^- cm^{-2}$	I_{sc} (mA)		V_{oc} (volts)		P_{ep} (mw)		P_{max} (mw)		Fill Factor	
	Solar Simulator	Tungsten Lamp	S S	T L	S S	T L	S S	T L	S S	T L
0	26.5	13.8	0.99	0.96	26.2	13.2	19.8	9.8	0.756	0.742
5.0×10^{14}	23.0	--	0.89	--	20.5	--	16.1	--	0.785	--
8.0×10^{14}	22.0	11.2	0.89	0.86	19.6	9.6	15.4	7.5	0.786	0.781
1.6×10^{15}	19.5	--	0.86	--	16.8	--	13.0	--	0.774	--
3.0×10^{15}	16.7	8.8	0.83	0.81	13.9	7.1	10.7	5.4	0.770	0.761

Table 5. Cell No. 9-15-75C

$e^- cm^{-2}$	I_{sc} (mA)		V_{oc} (volts)		P_{ep} (mw)		P_{max} (mw)		Fill Factor	
	Solar Simulator	Tungsten Lamp	S S	T L	S S	T L	S S	T L	S S	T L
0	37.3	14.5	0.95	0.91	35.4	13.2	18.9	8.5	0.534	0.644
5.0×10^{10}	36.7	--	0.89	--	32.7	--	16.5	--	0.505	--
9.6×10^{10}	33.5	13.5	--	0.81	--	10.9	--	6.9	--	0.633

Table 6. Cell No. 2-4-76B

$e^- cm^{-2}$	I_{sc} (mA)		V_{oc} (volts)		P_{ep} (mw)		P_{max} (mw)		Fill Factor	
	Solar Simulator	Tungsten Lamp	S S	T L	S S	T L	S S	T L	S S	T L
0	29.7	15.3	1.0	0.98	29.7	15.0	23.5	11.8	0.791	0.787
5.0×10^{10}	25.5	--	0.87	--	22.2	--	17.2	--	0.775	--
7.6×10^{10}	23.7	12.0	0.86	0.81	20.4	9.7	15.5	7.4	0.760	0.763
1.3×10^{11}	21.9	--	0.82	--	18.0	--	13.4	--	0.744	--
2.1×10^{11}	20.1	10.6	0.80	0.77	16.1	8.2	12.1	6.0	0.752	0.732
5.2×10^{11}	17.0	--	0.75	--	12.8	--	9.3	--	0.727	--

Table 7. Cell No. 1-30-76D

$e^- cm^{-2}$	I_{sc} (mA)		V_{oc} (volts)		P_{ep} (mw)		P_{max} (mw)		Fill Factor	
	Solar Simulator	Tungsten Lamp	S S	T L	S S	T L	S S	T L	S S	T L
0	33.8	14.0	0.97	0.93	32.8	13.0	26.6	10.5	0.811	0.808
1.3×10^{11}	32.5	--	0.94	--	30.6	--	23.8	--	0.778	--
2.6×10^{11}	--	13.1	--	0.89	--	11.7	--	8.9	--	0.761

Table 8. Cell No. 3-2-76A

$e^- cm^{-2}$	I_{sc} (mA)		V_{oc} (volts)		P_{ep} (mw)		P_{max} (mw)		Fill Factor	
	Solar Simulator	Tungsten Lamp	S S	T L	S S	T L	S S	T L	S S	T L
0	27.5	13.2	1.0	0.96	27.5	12.7	21.0	9.6	0.764	0.756
1.3×10^{11}	26.4	--	0.92	--	24.3	--	18.4	--	0.757	--
2.5×10^{11}	25.5	11.8	0.91	0.86	23.2	10.1	17.5	7.7	0.754	0.762
4.9×10^{11}	23.0	--	0.83	--	19.1	--	14.4	--	0.754	--
9.7×10^{11}	22.1	10.1	0.82	0.78	18.1	7.9	13.6	5.8	0.752	0.734
2.7×10^{12}	20.5	--	0.77	--	15.8	--	11.7	--	0.741	--

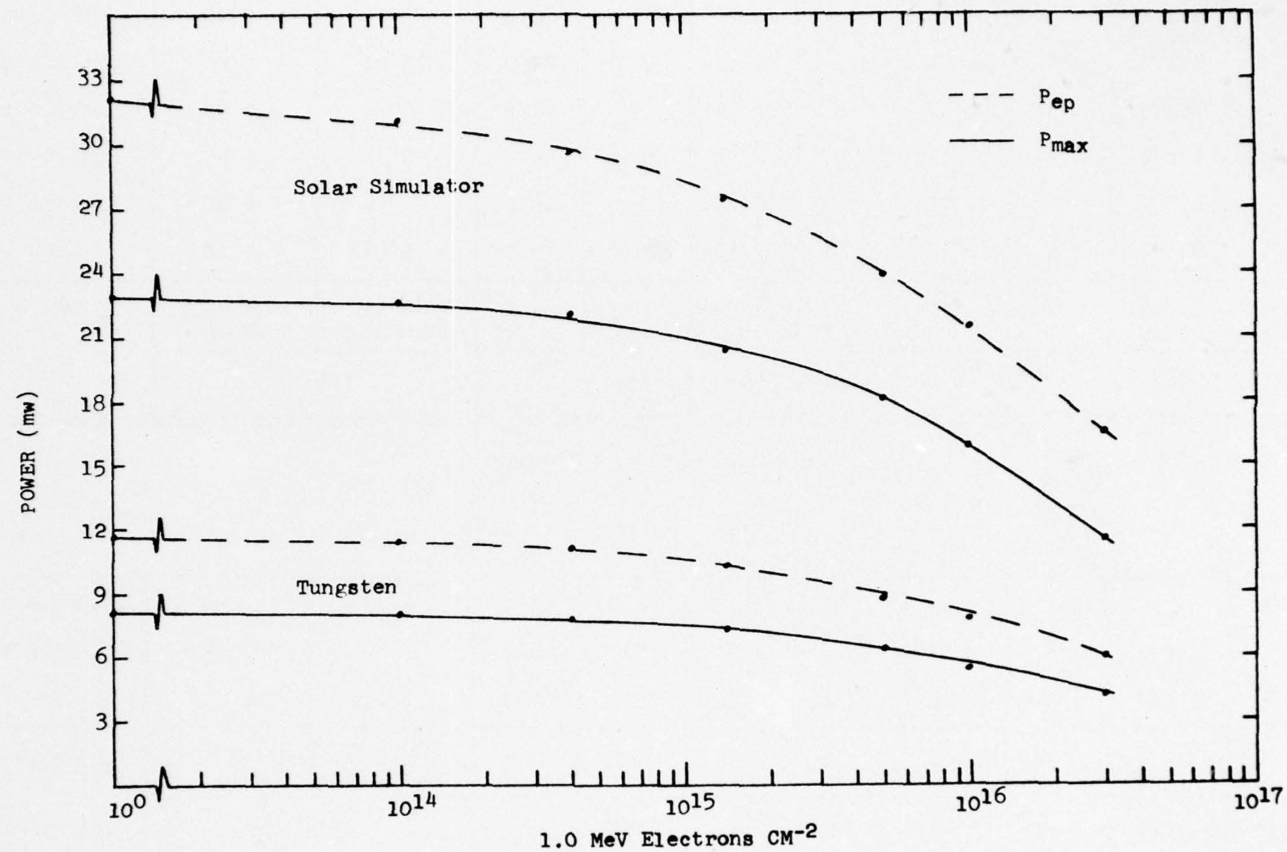

Figure 22. Power Curves of Cell No. 10-7-75B

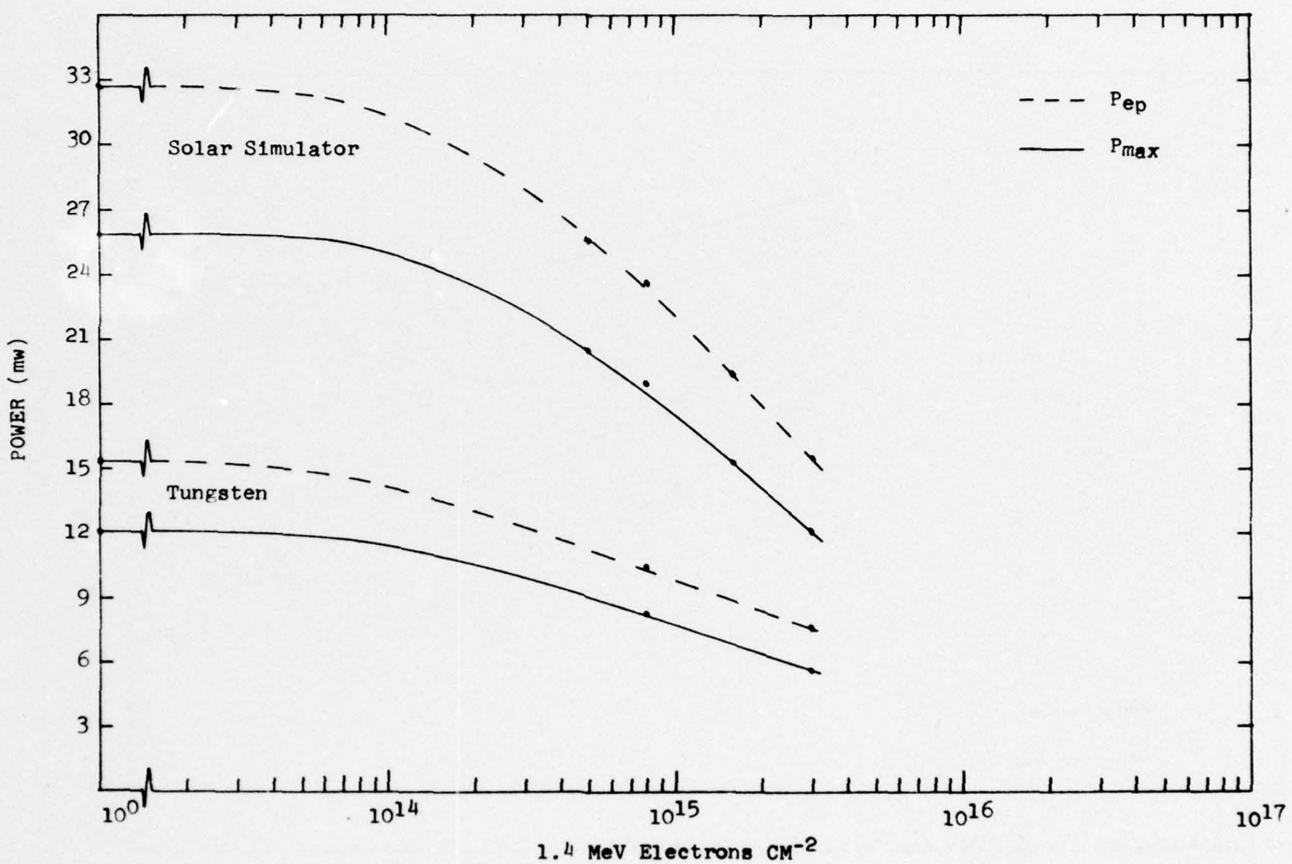

Figure 23. Power Curves of Cell No. 1-26-76B

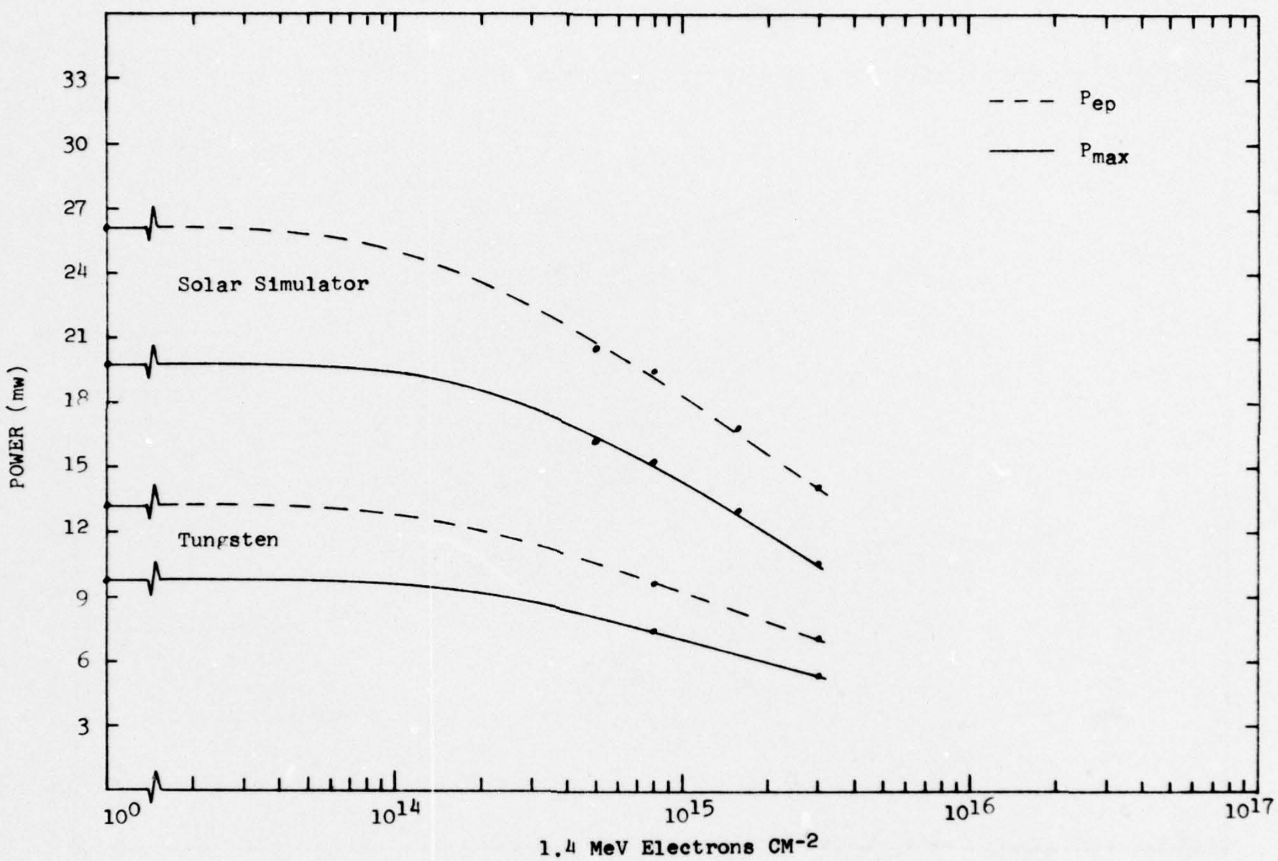

Figure 24. Power Curves of Cell No. 1-22-76B

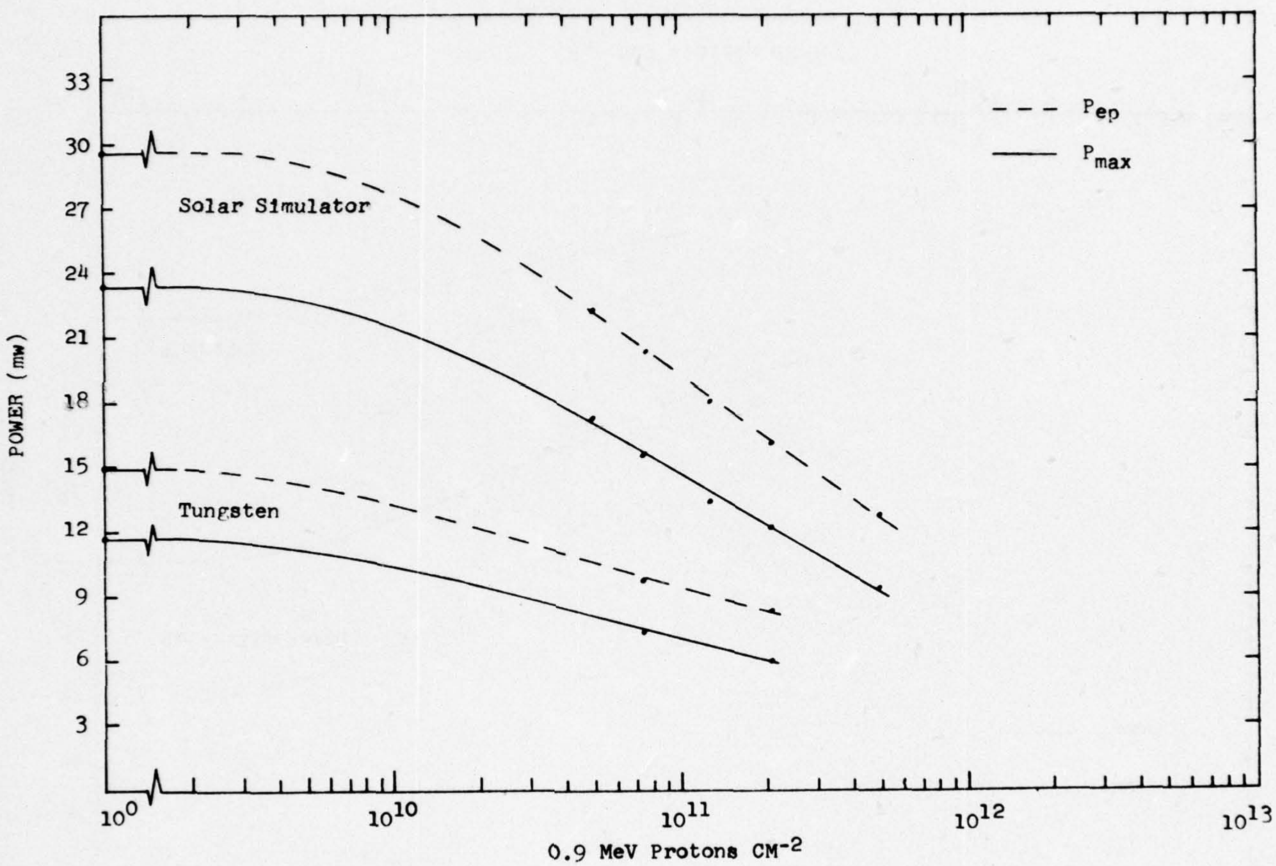

Figure 25. Power Curves of Cell No. 2-4-76B

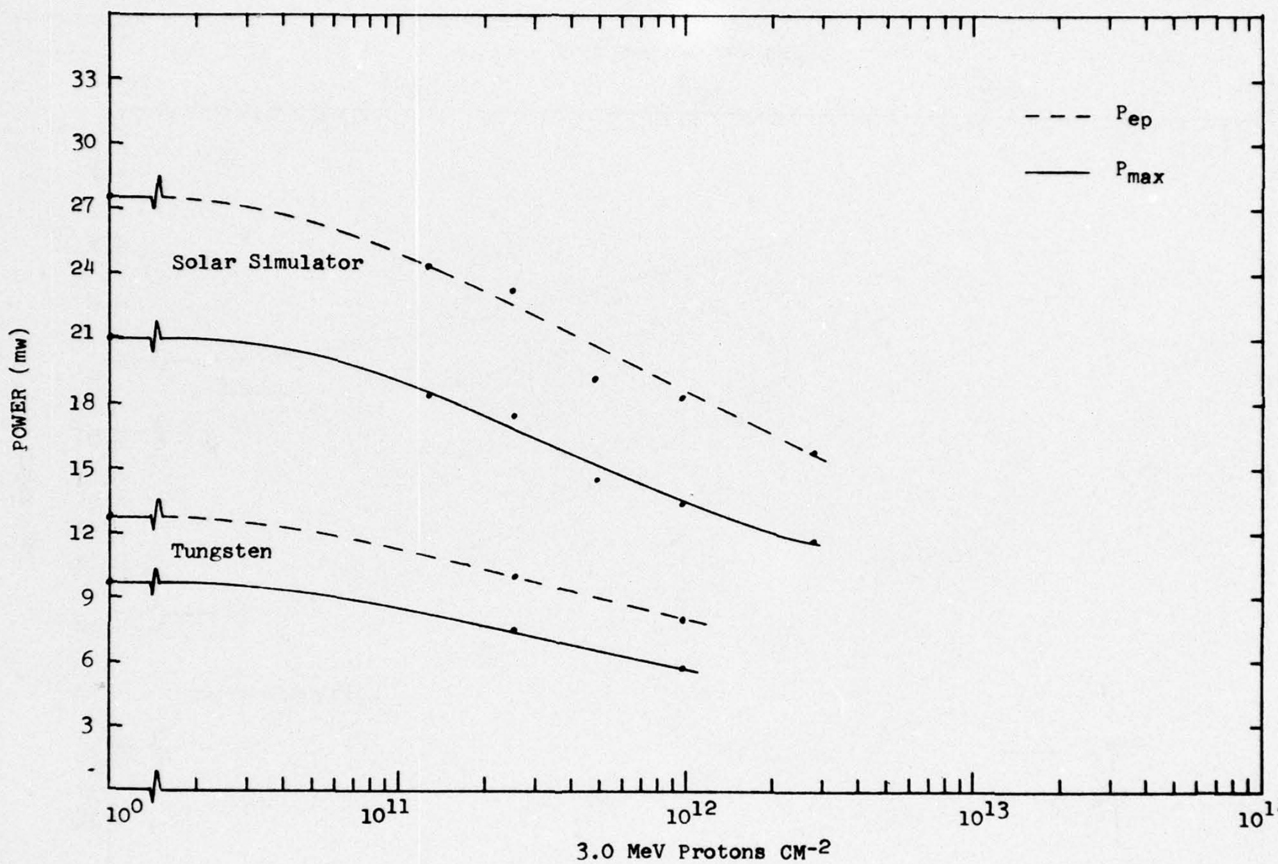

Figure 26. Power Curves of Cell No. 3-2-76A

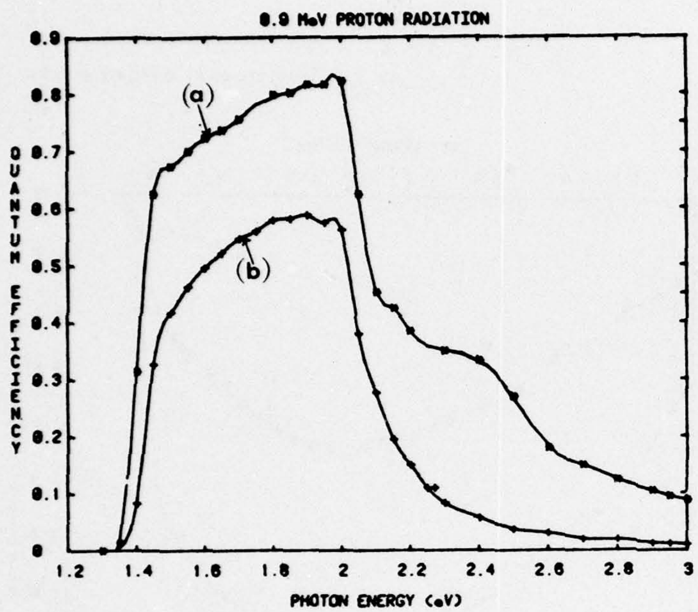

(a) * before irradiation, #2-476B

(b) + after irradiation to ∅ = 9.6×10^{10} p/cm^2

Figure 27. Spectral Response Curve for a Solar Cell Irradiated With 0.9-MeV Proton

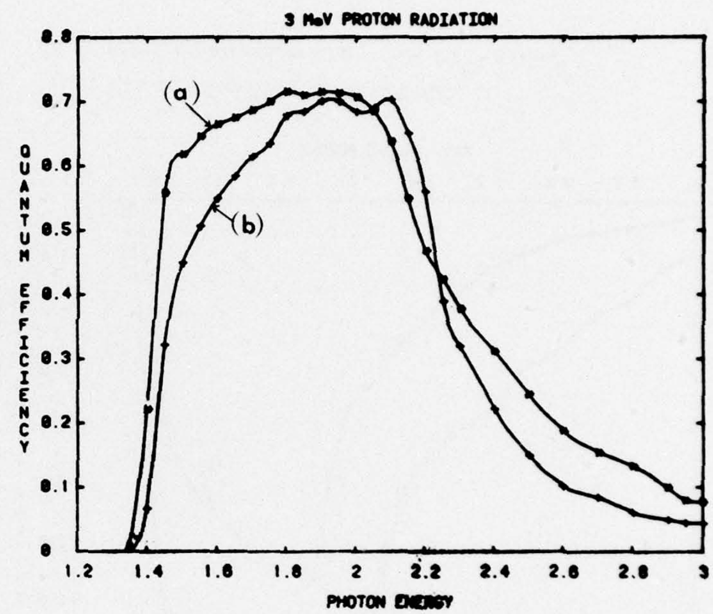

(a) * before irradiation, #3-276A

(b) + after irradiation to ∅ = 2.7×10^{12} p/cm^2

Figure 28. Spectral Response Curve for a Solar Cell Irradiated With 3-MeV Protons

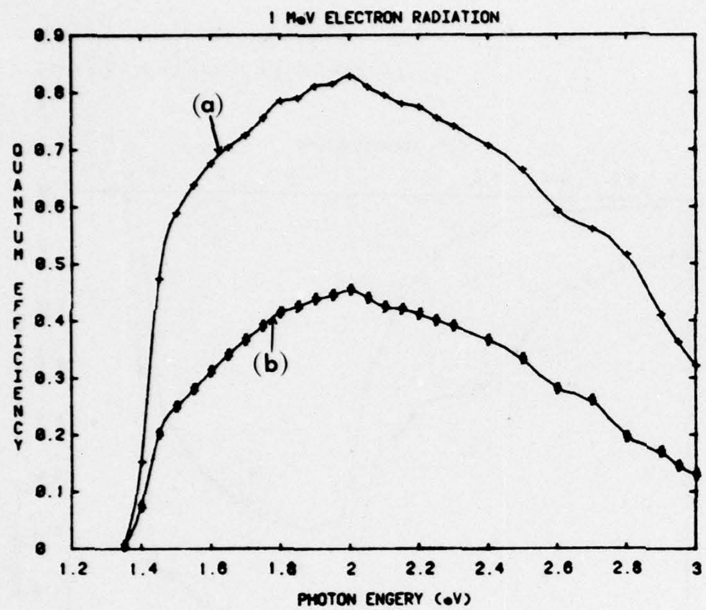

(a) * before irradiation, #9-2375B

(b) + after irradiation to $\phi = 3 \times 10^{16}$ e/cm^2

Figure 29. Spectral Response Curve for a Solar Cell Irradiated With 1-MeV Electron

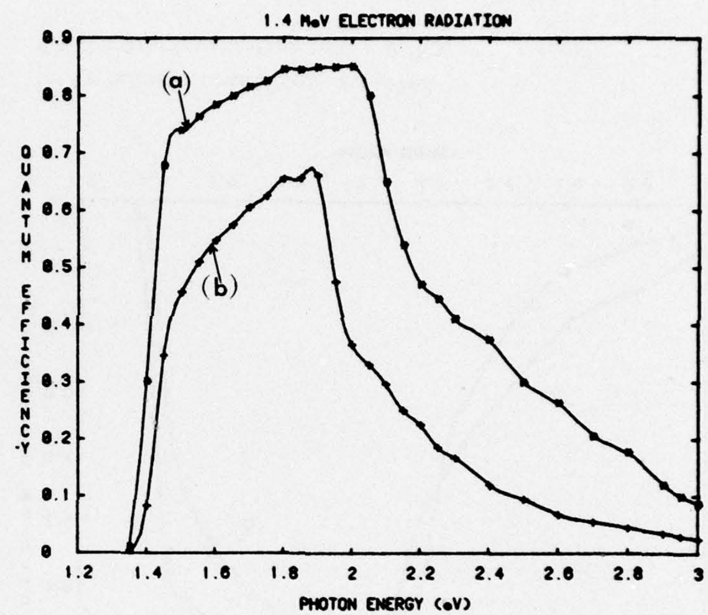

(a) * before irradiation, #1-2276B

(b) + after irradiation to $\phi = 3 \times 10^{15}$ e/cm^2

Figure 30. Spectral Response Curve for a Solar Cell Irradiated With 1.4-MeV Electrons

METRIC SYSTEM

BASE UNITS:

Quantity	Unit	SI Symbol	Formula
length	metre	m	...
mass	kilogram	kg	...
time	second	s	...
electric current	ampere	A	...
thermodynamic temperature	kelvin	K	...
amount of substance	mole	mol	...
luminous intensity	candela	cd	...

SUPPLEMENTARY UNITS:

Quantity	Unit	SI Symbol	Formula
plane angle	radian	rad	...
solid angle	steradian	sr	...

DERIVED UNITS:

Quantity	Unit	SI Symbol	Formula
Acceleration	metre per second squared	...	m/s
activity (of a radioactive source)	disintegration per second	...	(disintegration)/s
angular acceleration	radian per second squared	...	rad/s
angular velocity	radian per second	...	rad/s
area	square metre	...	m
density	kilogram per cubic metre	...	kg/m
electric capacitance	farad	F	A·s/V
electrical conductance	siemens	S	A/V
electric field strength	volt per metre	...	V/m
electric inductance	henry	H	V·s/A
electric potential difference	volt	V	W/A
electric resistance	ohm		V/A
electromotive force	volt	V	W/A
energy	joule	J	N·m
entropy	joule per kelvin	...	J/K
force	newton	N	kg·m/s
frequency	hertz	Hz	(cycle)/s
illuminance	lux	lx	lm/m
luminance	candela per square metre	...	cd/m
luminous flux	lumen	lm	cd·sr
magnetic field strength	ampere per metre	...	A/m
magnetic flux	weber	Wb	V·s
magnetic flux density	tesla	T	Wb/m
magnetomotive force	ampere	A	...
power	watt	W	J/s
pressure	pascal	Pa	N/m
quantity of electricity	coulomb	C	A·s
quantity of heat	joule	J	N·m
radiant intensity	watt per steradian	...	W/sr
specific heat	joule per kilogram-kelvin	...	J/kg·K
stress	pascal	Pa	N/m
thermal conductivity	watt per metre-kelvin	...	W/m·K
velocity	metre per second	...	m/s
viscosity, dynamic	pascal-second	...	Pa·s
viscosity, kinematic	square metre per second	...	m/s
voltage	volt	V	W/A
volume	cubic metre	...	m
wavenumber	reciprocal metre	...	(wave)/m
work	joule	J	N·m

SI PREFIXES:

Multiplication Factors	Prefix	SI Symbol
1 000 000 000 000 = 10^{12}	tera	T
1 000 000 000 = 10^{9}	giga	G
1 000 000 = 10^{6}	mega	M
1 000 = 10^{3}	kilo	k
100 = 10^{2}	hecto*	h
10 = 10^{1}	deka*	da
0.1 = 10^{-1}	deci*	d
0.01 = 10^{-2}	centi*	c
0.001 = 10^{-3}	milli	m
0.000 001 = 10^{-6}	micro	μ
0.000 000 001 = 10^{-9}	nano	n
0.000 000 000 001 = 10^{-12}	pico	p
0.000 000 000 000 001 = 10^{-15}	femto	f
0.000 000 000 000 000 001 = 10^{-18}	atto	a

* To be avoided where possible

MISSION
of
Rome Air Development Center

RADC plans and conducts research, exploratory and advanced development programs in command, control, and communications (C^3) activities, and in the C^3 areas of information sciences and intelligence. The principal technical mission areas are communications, electromagnetic guidance and control, surveillance of ground and aerospace objects, intelligence data collection and handling, information system technology, ionospheric propagation, solid state sciences, microwave physics and electronic reliability, maintainability and compatibility.

Printed by
United States Air Force
Hanscom AFB, Mass. 01731